RECENT DEVELOPMENTS IN HIGH-RESOLUTION NOBLE-LIQUID COUNTERS

Stephen E. Derenzo, Dennis B. Smith, Robert G. Smits,
Haim Zaklad, and Luis W. Alvarez
Lawrence Radiation Laboratory

and

Richard A. Muller
Space Sciences Laboratory, University of California, Berkeley

ABSTRACT

In an effort to develop a liquid-filled high-resolution wire chamber, we have studied the multiplication of ionization electrons in liquid argon and liquid xenon near the surface of fine wires from 3.5 to 13 μ in diameter and near etched tungsten tips from 1 to 2 μ in diameter. The pulse height and shape depend on the applied voltage and (in liquid argon) on the hydrostatic pressure. The pulses are 10^{-12} to 10^{-10} coulombs in size with a rise time of 5 to 10 μsec in liquid argon and < 5 nsec in liquid xenon.

Using a 3.5-μ tungsten wire in very pure liquid xenon, we have obtained our best results: a charged-particle detection efficiency greater than 30% and a time resolution of 100 nsec. In addition, a 3.5-μ wire in liquid xenon acts as a dc spark counter, delivering pulses 100 nsec wide and 5 to 10 V high into a 50-ohm load. With somewhat larger wires or when liquid argon is used, electron avalanching is unreliable and occurs at places only sparsely distributed along the length of the wire.

In order to develop a practical high-resolution counter, we propose to use conducting strips attached to a dielectric substrate. We show how it is even possible to deposit a row of sharp points on each conducting strip. We also present a new scheme that should be capable of automatically reading out thousands of closely spaced conductors.

I. INTRODUCTION

This paper describes the progress we have made toward realization of a high-spatial-resolution detector using noble liquids. In Section II we show a calculation of momentum error for several spectrometers, indicating how noble-liquid detectors can be used to achieve high-momentum resolution. In Sections III and IV we show how our techniques have advanced since our last report.[1] We have studied electron amplification

in liquid argon, both on fine wires (Section V) and on sharp points (Section VI). Section VII presents some preliminary results in liquid xenon, and in Section VIII we present a scheme for building orderly arrays of points and reading them out.

II. ACHIEVING HIGH SPATIAL RESOLUTION

As we probe the structure of matter at higher and higher energies, it becomes advantageous to use a particle detector that has the automatic readout of the wire spark chamber but a greatly improved spatial resolution. Figure 1 shows the advantages in spectrometer size gained by using a high-resolution detector. Curve A shows the momentum resolution as a function of momentum for a large conventional spectrometer with 20 kG-meters of magnetic field, 1-meter spacing between detector planes, and 250-μ spatial resolution. Below 12 GeV/c the momentum determination is better than 1%. To maintain the same momentum resolution at 120 GeV/c, one can either triple the magnetic-field integral and triple the spacing between chamber pairs (curve B) or use a detector with 25-μ spatial resolution (curve C). For many experiments it will be impossible to triple the linear dimensions of the experimental apparatus, and a detector with 25-μ or better spatial resolution becomes necessary.

The discovery[1] of electron avalanche in the noble liquids makes possible, we believe, a particle detector with a thickness of 100 μ or less, with a spatial resolution of ± 10 μ. Such a detector would introduce ≤ 0.005 radiation lengths. The anode plane would consist of an insulating sheet supporting many conducting strips, each with a width of a few μ, spaced about 20 μ apart.

III. EXPERIMENTAL PROCEDURE

Our work so far has involved chambers consisting of single wires and single points in liquid argon and liquid xenon. One year ago we reported[1] on the characteristics of single-wire chambers in liquid argon. Since that time, by improving our experimental techniques we have significantly improved the performance of our chambers and the reproductibility of their behavior. In this section we discuss these techniques in detail.

Chamber Construction

Figure 2 shows the construction of a single-wire cylindrical chamber. The glass-to-metal joints are Kovar seals, and stainless steel tubing is used for the rest of the chamber. Every time a central electrode is installed the chamber is washed with a series of solvents (trichlorethylene and ethyl alcohol) in an ultrasonic cleaner and baked in an oven at 110° C for 10 min.

The single-point chambers are similar, except that a tungsten needle is supported from the upper connector so that its point is located near the center of the cathode region.

Vacuum Pumpout

The chambers were evacuated to $< 2 \times 10^{-6}$ mm Hg by pumping overnight at room temperature with a mercury diffusion pump, and then were valved off for 30 min. During this period the chamber pressure was monitored with a Philips ionization gauge to estimate the vapor pressure of any contaminants. In the absence of a leak, the pressure always reached a steady state within 15 min. The vapor pressure was almost always below 10^{-4} mm Hg and was quite often below 5×10^{-6} mm Hg.

Gas Preparation

The purification system is designed to reduce the electronegative impurity gases in the stream of noble gas, specifically argon and xenon, to a small fraction of a part per million. The argon used is supplied by a commercial vendor in a standard 200-ft^3 tank, and the xenon is supplied in smaller tanks containing 1 ft^3. The purifier is capable of removing O_2, N_2, CO, CO_2, and water. At present we are capable of monitoring the oxygen content of argon to an accuracy of about 100 parts per billion, using a Beckman Model 80 oxygen analyzer. In the future, with the aid of a Varian model 1732-2B gas chromatograph, we will be able to monitor the other impurities to a similar accuracy.

The argon-purifier block diagram is shown in Fig. 3. The gas is circulated continuously through the purifier by a small positive displacement pump (Air Control Inc. model 08-800-70, Norristown, Pa.). The total volume of the system is about 4 liters. Argon supplied at 2.5 ppm O_2 impurity is reduced by our purifier to 100 ± 50 parts per billion in less than 8 min.

A separate xenon-purification system was built containing only calcium chips and Linde molecular sieve 4A. Once pressurized, the system is capable of filling our chambers with pure xenon and then emptying them without any loss of xenon.

For further details concerning the purifier and its operation, see Appendix B.

Refrigeration

Purified gaseous argon is condensed in the chambers by immersion in a bath of boiling liquid argon (available at a cost of $26 per 100 liters). Purified gaseous xenon is condensed in the chambers by immersion in melting Freon-11. The Freon-11 is kept cold by means of coils carrying liquid nitrogen. A xenon vapor-pressure thermometer controls the flow of liquid nitrogen through the coils.

IV. IONIZATION PULSES IN LIQUID ARGON

If more than about 100 keV is deposited in our chamber by ionizing radiation and the liquid is sufficiently pure, it is possible to observe the liberated electrons, with the help of a charge-sensitive amplifier (gain of 0.4 V/pC). These ionization pulses

are due to the motion of free electrons toward the positive electrode (anode). In Fig. 4 we show a pulse-height distribution for Compton electrons produced in the chamber (see Fig. 2) by 1.1-MeV gamma rays from a ^{65}Zn source. The deviation from the predicted curve is probably due to the loss of energetic Compton electrons from the chamber before the end of their range.

The size of the ionization pulses from a standard source is the best gauge of the purity of the liquid.* Electronegative impurities capture the electrons to form heavy negative ions which, because of their low mobility, are not observed. Figure 5 shows the correlation between oxygen impurity (as measured on our Beckman 80 analyzer) and ionization pulse size. Oxygen concentrations of 1 ppm drastically reduce pulse size. For thinner chambers larger concentrations of impurities could be tolerated, perhaps as much as 50 ppm for a 100-μ thick chamber.

Since a minimum-ionizing particle loses only 21 keV when traversing 100 μ of liquid argon, multiplication in the liquid is essential for a practical high-resolution detector.

V. AVALANCHE PULSES NEAR FINE WIRES IN LIQUID ARGON

Amplified pulses occur when free electrons gain sufficient energy from the electric field to ionize argon atoms, producing more free electrons. We have observed such amplification to take place near the surface of fine wires when the calculated field strength is of the order of 2×10^6 V/cm and the gas purity is better than several ppm. Unlike the ionization pulses, however, the avalanche pulses usually have a very narrow pulse-height distribution, as if there were some sort of saturation process taking place (see Fig. 6). We have only rarely seen pulses that had enough variation in size to indicate that proportional multiplication might be occurring. The efficiency of our counter, defined as the ratio of avalanche pulses to ionization pulses, has always been low, never greater than about 20%.

Moreover, it appears that the amplification process on fine wires in liquid argon is unreliable.[3] Fluctuations in the count rate are observed on time scales of seconds, minutes, and even hours. This is true even when external variables such as temperature, pressure, and voltage are rigorously held constant. There are also periods when the counter is "dead," with no detectable source effect.

Hot Spots

In order to investigate the low counting efficiency of the wire, we built a collimated ^{241}Am source. This source, a brass cylinder with 6-mm-thick walls and a

*Recombination is unimportant at the fields we work with. The fraction surviving recombination is approximately $1/(1+k/E)$ for minimum ionizing particles,[2] where $k = 1.1 \pm 0.2$ kV/cm and E is the electric field.

2-mm opening at one end, provided a beam of 60-keV x rays that was 3 mm in diameter when it reached the chamber. With this source we found that only certain regions of the wire could cause an avalanche. These regions are usually quite narrow (see Fig. 7), although they have been seen 1 cm wide.

These "hot spots" can appear and disappear over the passage of time, after sparking, or after the argon has been dumped and replaced with freshly prepared argon (compare Figs. 7A and 7B). As Fig. 7 shows, some hot spots are more persistent than others. We have built a chamber in which the central wire can be moved a few mm with respect to the cathode and have found that the hot spots move as the wire is moved. But although the hot spots must be associated with some feature of the wire, we have been unable to determine what that feature is. Microscopic examination of these regions both during running (≈ 4 μ visual resolution) and after dumping and warming (≈ 2 μ visual resolution) reveals, at most, very small pieces of dust, no different in appearance from those seen all along the wire. Our 13-μ-diam stainless steel wires do not show imperfections, even when viewed with the scanning electron microscope (see Fig. 8). The surface roughness has also been measured (indirectly) by reversing the voltage, making the wire negative with respect to the outer cylinder. Field emission is not observed until the surface reaches a field of 1 million V/cm (calculated by assuming the wire to be a perfect cylinder), which is as high as that achieved by most smooth metal surfaces.[4]

We have never been able to control the number of hot spots that appear on our wires, or their positions. They have been an unreliable phenomenon associated with the wire and possibly due to impurities or very small imperfections. We have attempted to increase the efficiency (i.e., the number of hot spots) by raising the voltage, but found that if the voltage is increased much above that needed for avalanche pulses, we observe spontaneous spark breakdown all along the length of the wire.

Sparks

The sparks are quite audible and bright and show no dependence on the presence of ionizing radiation. We do not understand the mechanism of this breakdown. Cathode field emission by itself does not seem to be the cause of the sparking, since when we replace the fine-wire anode with a much larger wire, the sparks do not occur, even for higher cathode fields. If, through some mechanism, a few electrons are liberated into the liquid, then perhaps a combination of anode-cathode effects can lead to breakdown, as discussed by Swan and Lewis.[5]

As mentioned in Ref. 1, we observe that the height of the avalanche pulses in liquid argon is a function of the hydrostatic pressure. Figure 9 shows this dependence. We shall discuss this dependence further in Section VI.

VI. AVALANCHE PULSES FROM SHARP POINTS IN LIQUID ARGON

Motivation for Using Points

According to the work of E. W. Müller and K. Bahadur,[6] argon gas is ionized in the presence of electric fields of the order of 100 million V/cm. Bob Henson[7] has repeated some of Müller's experiments in liquid argon, and although he has no direct measurement of the electric field strengths on the tips of his chemically etched tungsten points, he concluded that field ionization in the liquid is essentially the same as that in the gas. Since Henson claimed to be able to hold off 100 million V/cm in the liquid, and our wires were supporting only a few million V/cm, we decided to repeat Henson's experiment using our chamber geometry and our liquid argon, but substituting a point for a wire.

Point Construction

Our tungsten points were made by following the procedures described by E. W. Müller.[8] A tungsten wire, 0.005 in. in diameter, or a tungsten rod, 0.060 in. in diameter, is dipped in a dilute solution of sodium hydroxide. A nickel electrode is also dipped in the solution, and a 5- to 10-V ac current is passed between the nickel electrode and the tungsten rod. Within a few minutes the tungsten has been etched to a tip radius that cannot be resolved with an optical microscope. In Fig. 10 we show a typical tip, etched from a 0.060-in. tungsten rod and magnified with a scanning electron microscope.

These tips, when immersed in liquid argon, drew currents of < 1 nA when voltages > 3000 V were applied to them--results similar to Henson's. To our amazement, we discovered that when we brought a ^{65}Zn source of 1.1-MeV gamma rays near the tip, we detected avalanche pulses. A collimated source 3 mm in diameter proved that the avalanching was indeed taking place only in the region of the tip. At the time of this writing we have run eight such tips, and all eight have successfully produced avalanche pulses.

Stability and Lack of Time Variation

The appearance of the pulses produced by these point counters is similar to that of the pulses seen with the wire chambers. The pulse height of the pulses vs voltage is shown in Fig. 11. The pulse height varies roughly as the third power of the voltage. This dependence might be due to the increase in length with voltage of the section of the tip that has sufficiently high field to cause avalanche. The count rate vs voltage is shown in Fig. 12. The increase of count rate with voltage may be due to the increasing sensitive volume of the chamber. The pressure dependence of the pulse height is shown in Fig. 9.

Pressure Dependence of Pulse Size and Shape

One of the greatest mysteries associated with electron multiplication in liquid argon is that the pulse size and shape depend on the hydrostatic pressure. Figures 13 and 14 show two types of pulses, both of which have been observed on points in liquid argon, at times concurrently. The first type rises in about 5 μsec and has a fall time that is determined by the 100-μsec differentiation. The second type of pulse has an additional constant-current component which rises in about 100 μsec, lasts anywhere from 1 to 20 msec, and then ends abruptly. As can be seen in Figs. 13 and 14, the height of the first type of pulse is sharply reduced by an increase in hydrostatic pressure, whereas the height of only the initial rise of the second type of pulse depends upon the pressure.

The pressure dependence, together with the existence of hot spots, suggests the existence of microscopic bubbles adhering to the wire with avalanche taking place in the gas. A "bubble theory" must answer the following objections:

1. How can the bubbles coexist with the liquid at several atmospheres pressure at 87° K? (The avalanche itself does not release enough energy to vaporize the liquid.)

2. Why do we observe no avalanche at fields below 3×10^5 V/cm? (In the gas at 1 atm, avalanche occurs at fields lower than 10^4 V/cm.)

3. The bubbles must be smaller than 4 μ in size. (We have observed our points with a microscope while running, with 4-μ resolution, and failed to observe bubbles.) Yet if the bubbles are much smaller than 1 μ, there simply are not enough atoms in the bubble to give our picocoulomb signals.

4. When the wire is heated by passing a small current through it, no change in pulse size is observed.

While we feel that the bubble theory is inadequate, we have no alternative theory to present.

Sparking from Sharp Points in Liquid Argon

Sharp points in liquid argon have acted as dc spark counters, delivering pulses as high as 60 V into a 125-ohm load, an order of magnitude larger than similar sparks in liquid xenon (see Section 7). These pulses rise in 50 nsec and have a width of 200 nsec. The potential required for this mode of operation is somewhere around 7000 V.

VII. PRELIMINARY RESULTS IN LIQUID XENON

Avalanche Pulses

We have made several runs using liquid xenon instead of liquid argon, with surprising and important results. Using both etched tungsten tips and 3.5-μ-diam tungsten wires,[9] we have observed avalanche pulses in liquid xenon, at approximately the

same fields as necessary for avalanche in liquid argon. But the avalanche pulses in liquid xenon have a much higher efficiency and a rise time of less than 5 nsec, indicating a very high positive-charge mobility (perhaps due to hole conduction). This fast rise time has practical consequences for chambers with good time resolution.

The best efficiency and reliability have been observed by using 3.5-μ wires in very pure liquid xenon. In six runs, using three different sections of wire, the efficiency was observed to be much higher than that of our argon counters.

Because of the difficulties in determining efficiency when using a gamma-ray source, at this time all we can say is that we believe the efficiency is better than 30%, and perhaps near 100% for parts of the wire. The operation of the wire was not quite as stable as that of our 2-μ-diam points (nonstatistical fluctuations in count rate were observed), but we hope to improve the performance by using purer liquid and finer electrodes.

Time Resolution

For a multiwired chamber with a scanned readout (see Section 8), the time resolution is in part determined by the rise time of the pulse. Therefore the fast rise time observed in liquid xenon offers the possibility of a chamber with good time resolution as well as good spatial resolution.

We have determined the timing characteristics of the liquid xenon wire (3.5-μ-diam) chamber by using the two colinear gamma rays from a ^{22}Na positron source. One gamma ray was detected in a plastic scintillator and the other was detected in an 8-mm-diam single-wire xenon chamber (see Fig. 15). The xenon avalanche pulse was found to occur (on the average) 100 nsec after the passage of the particle, with a jitter of 100 nsec (see Fig. 16). If this jitter is due to variations in electron transit time to the anode, we expect that the time resolution will be correspondingly better in thin (100-μ) chambers.

Sparking

When we raise the dc voltage above that necessary for avalanche, we find a narrow band of voltages (usually near 5 kV) for which the wire chamber behaves as a low-efficiency dc spark counter. The sparks are relatively low energy (they don't seem to damage the 3.5-μ wire), are less than 200 μ in diameter, and follow a collimated 60-keV x-ray source as it is moved along the wire. The pulses produced on the anode wire by these sparks are 100 nsec wide and 5-10 volts high into a 50-ohm load. Because of the simplification in readout afforded by such a large output pulse, we shall try to increase the efficiency in the spark mode by pulsing the chamber to higher voltages. Even when the dc breakdown voltage is only 5 kV, we have found that the chamber can be pulsed to 10 kV (for 1 μsec) without spontaneous breakdown.

VIII. THOUGHTS ON PRACTICAL HIGH-RESOLUTION CHAMBERS

Conducting Strips on Glass and Mylar

In order to develop a practical high-resolution counter, we propose to use conducting strips attached to an insulating substrate. Corporations such as Buckbee-Mears can inexpensively produce a 6 × 6-in. pattern in chrome (with a resolution of 2 μ) bonded to a sheet of glass. It is important to realize that so far as conducting lines are concerned, integrated-circuit techniques can be applied on a large scale. In the following section we discuss how it is even possible to deposit a row of sharp points on each conducting strip.

Deposition of Arrays of Points

Several days after discovering the ease with which points can be made to produce avalanche multiplication, we received a letter from Don Cone of the Stanford Research Institute. He wrote that it is within current technology to produce arrays of points with tip radii of only a few thousand angstroms and precise 25-μ spacing between tips. Scanning electron micrographs of such arrays are shown in Fig. 17. These arrays are made by a simple but ingenious technique. A screen with square holes at 25-μ spacing (manufactured inexpensively by Buckbee-Mears, St. Paul, Minn.) is placed over an insulating substrate. A tungsten-alumina or chromium-alumina alloy is then vapor-deposited through the screen onto the substrate. The substrate is plated with the images of the holes, and as the holes clog up, smaller and smaller squares are plated, until the holes in the screen are completely filled, and on the substrate we are left with the pyramid-like structures shown in Fig. 17. There should be little difficulty in making large arrays by use of this technique. Likewise, by spacing the screen several mils above the substrate, and by moving the source during the initial stages of deposition, long rows of these pyramids can be electrically connected. We shall soon be using pyramid arrays in our chambers in order to look for avalanche multiplication at the tips. The fields at the tips of the pyramids must be great enough to produce electron avalanching, yet the field at the opposing plate must be lower than the field necessary to produce field emission. In Fig. 18 we show the electric field enhancement factor for a spheroidal structure placed on a flat plate.[10]

Readout

A more detailed discussion is given in Ref. 11; a brief summary follows. With recent advances in large-scale integration of solid state circuits, large arrays of closely spaced wires can be automatically scanned. The charge level deposited on a wire in the noble liquid detector is on the order of 1 to 100 picocoulombs, well above the switching noise of a device that we shall now describe.

Fairchild Semiconductor Division has developed a self-scanned 48-photodiode array, the FPA 600. The diodes are spaced 200 to the inch, and each is connected to an FET switch. A self-scan generator, integrated on the same chip, controls the FET switches. When a switch is turned on, the charge developed at the diode appears on a common drain line. A driving frequency of 1 MHz and a start pulse are supplied from the outside to drive the switches consecutively. When a switch is "off," the leakage from its input line is 0.1 pA. The minimum detectable signal (limited by the switching noise) is 2×10^{-2} pC. Fairchild is presently considering making 128 switches per chip.

From the discussion with Fairchild representatives, it appears that a rather minor change would be required to modify their device to suit our requirements. By altering the mask used in the production of this chip, a metallic bonding pad can be connected to each FET switch in place of the photodiodes (see Ref. 11, Fig. 2) so that it becomes an "electronic rotary switch." The applications of this device extend far beyond those of the noble-liquid detector. The readout of other multiwire counters is one type of direct application. We estimate that the price can be reduced in the near future to less than $0.30 per switch, providing there is a large enough demand. We should keep in mind that this cost includes the complete driving circuit for each switch.

Several of these devices can be connected in series to provide a self-scanned array with size limited only by the time resolution required. For example, in a cosmic-ray experiment or in an accelerator experiment with particle traversals below 50 per second, a counter of 5120 wires in which 40 self-scanned devices are connected in series would require 5.12 msec to drive the data into a computer memory with relatively little additional control logic.

If better time resolution is required, then an additional integrated circuit is necessary (see Ref. 11, Fig. 3), having the following properties:

1. All charge on the wires will be leaked to ground with a time constant of about 100 nsec.

2. Whenever an event is identified (and before all the charge has leaked to ground) all lines are briefly connected to individual storage capacitors. These capacitors can then be read out by the self-scanned array mentioned above.

With this scheme, the time resolution of the detector should be somewhat better than that of present-day spark chambers.

Acknowledgments

We are indebted to Buck Buckingham, Joe Savignano, Tony Vuletich, and Todd Hauser for help in all phases of this work. We are grateful to Carl Pennypacker,

Serban Protopopescu, and Gerard Smadja for assistance during the design and data-taking phases of this work. We thank Roger Hildebrand, Wulf Kunkel, Sam Lindenbaum, Mike Neuman, and Pete Schwemin for helpful discussions. The scanning electron micrographs of our fine wires and etched tungsten tips were made possible through the cooperation of George Georgakopoulos of the Inorganic Materials Research Division at LRL-Berkeley. We also wish to thank Don Cone, Lou Heynick, and Capp Spindt of the Stanford Research Institute for their cooperation in providing us with pyramid arrays and the marvelous scanning electron micrographs of these arrays.

REFERENCES

[1] Stephen E. Derenzo, Richard A. Muller, Robert G. Smits, and Luis W. Alvarez, The Prospect of High Spatial Resolution for Counter Experiments: A New Particle Detector Using Electron Multiplication in Liquid Argon, Lawrence Radiation Laboratory Report UCRL-19254, 1969; published in National Accelerator Laboratory 1969 Summer Study Report SS-154, Vol. III, pp. 79-102.

[2] John Marshall, Rev. Sci. Instr. 25, 232 (1954).

[3] Roger Hildebrand's Group at the University of Chicago has come to the same conclusion (private communication).

[4] D. W. Swan, Proc. Phys. Soc. (London) 78, 423 (1961); D. W. Swan and T. J. Lewis, Proc. Phys. Soc. (London) 78, 448 (1961).

[5] D. W. Swan and T. J. Lewis, J. Electrochem. Soc. 107, 180 (1960).

[6] Erwin W. Müller and Kanwar Bahadur, Phys. Rev. 102, 624 (1956).

[7] Bob L. Henson, Phys. Rev. 135, A1002 (1964).

[8] L. Marton, Ed., Advances in Electronics and Electron Physics, Vol. XIII (Academic Press, Inc., New York, 1960), p. 129.

[9] Produced in a special experimental run by the Philips Elmet Corp., Lewiston, Maine.

[10] F. M. Charbonnier and L. N. Heynick, 21st Annual Conference on Physical Electronics, MIT, 1961. The field-enhancement factor for a conducting structure attached to one of two parallel conducting planes is the ratio of the maximum field at the surface of the structure to the field that obtains when the structure is removed.

[11] Haim Zaklad, Integrated Circuit Readout for Closely Spaced Wire Arrays, Lawrence Radiation Laboratory Report UCRL-20123, July 1970, National Accelerator Laboratory 1970 Summer Study Report SS-213, Vol. I, p. 75.

[12] BASF Colors and Chemicals, 845 Third Ave., New York, New York 10022.

APPENDIX A. SOME USEFUL FACTS ABOUT ARGON AND XENON

	Argon	Xenon
Boiling point at 1 atm (° C)	-185.7	-107.1
(° K)	87.4	166
Melting point at 1 atm (° C)	-189.2	-111.9
(° K)	83.9	161.2
Density of liquid (g/cc)	1.40 (-186° C)	3.06 (-109° C)
Density of solid (g/cc)	1.65 (-233° C)	2.7 (-140° C)
Density ratio, liquid/gas, at 1 atm	785	523
Ionization potential (eV)	15.76	12.13
Energy loss per 100 μ (keV) (minimum ionizing radiation)	21	43
Ion pairs per 100 μ (minimum ionizing radiation)	810	Approx 1500
Fraction of a radiation length per 100 μ	0.00067	0.0044
Cost of gas (at standard temperature and pressure)	$80 per 200 ft^3 (< 1 ppm impurity)	$25 per liter
Suitable refrigerant	Boiling liquid argon	Melting Freon 11
Refrigerant cost	$26 per 100 liters	$77 per 15-gal drum

APPENDIX B. NOBLE-GAS PURIFICATION SYSTEM

The noble gas purification system used in our work is shown in Fig. 3. The total volume of the system is 4 liters. The system consists of four chemical-reaction tanks plus two 1-liter ballast tanks. The space velocity of a reactor is defined as R/V, where R is the flow rate in liters per hour and V is the volume in liters. At a flow rate of 2 liters/min the space velocity of our purifier is less than 500 per hour per pass in all stages.

The first stage consists of Linde molecular sieve 4A, at room temperature, which removes water by adsorption. The second stage is a reactor containing calcium turnings and is maintained at 660° C. Here, the oxygen and nitrogen are removed according to the reactions

$$2\ Ca + O_2 \rightarrow 2\ CaO, \quad 151.0\ kcal/mole,$$

$$3\ Ca + N_2 \rightarrow Ca_3N_2, \quad 103.2\ kcal/mole.$$

When the freshly charged turnings are heated, the water adsorbed at their surface is released. In the presence of calcium the water is broken into free oxygen and hydrogen.

Therefore fresh calcium chips must be heated and pumped on before they can be used to purify gas.

The third stage is a reactor containing an active copper-catalyst preparation maintained at 180° C. This material, called BTS, is produced by the Badische Aniline und Soda-Fabrik.[12] The main reaction is

$$2\ Cu + O_2 \rightarrow 2\ CuO, \quad 31.1\ kcal/mole.$$

When H_2 or CO is present, the following reduction reactions occur:

$$CuO + CO \rightarrow Cu + CO_2,$$

$$CuO + H_2 \rightarrow Cu + H_2O.$$

The latter reaction is used in two ways: to remove the hydrogen released in the previous stage and (in a separate operation) to occasionally regenerate the BTS. Regeneration is accomplished by passing a mixture of 4% H_2 and 96% He over the hot BTS pellets. When the copper is reduced, the released water is removed by heat and evacuation.

The fourth stage contains molecular sieve 4A at dry ice temperature. This serves to trap the remaining water left over after the regeneration of the BTS and to remove CO_2 and hydrocarbons from the system.

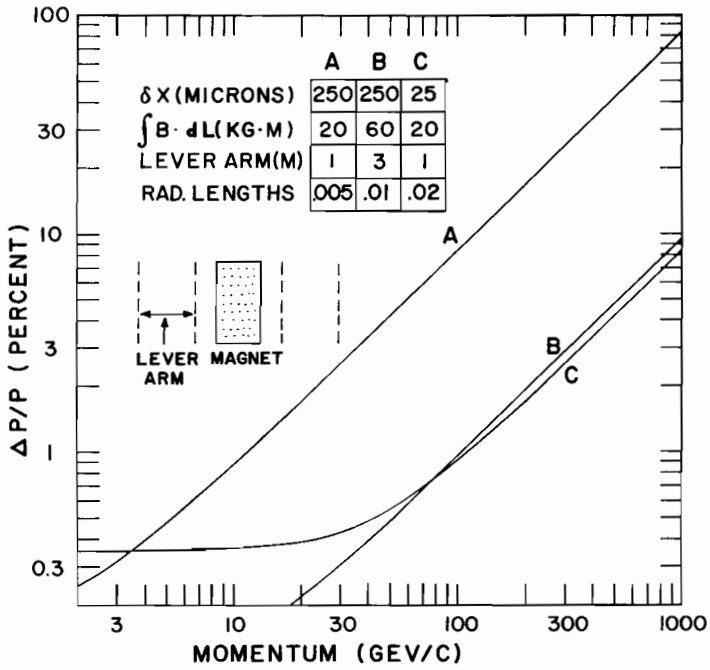

Fig. 1. Comparison between three spectrometers (see text).

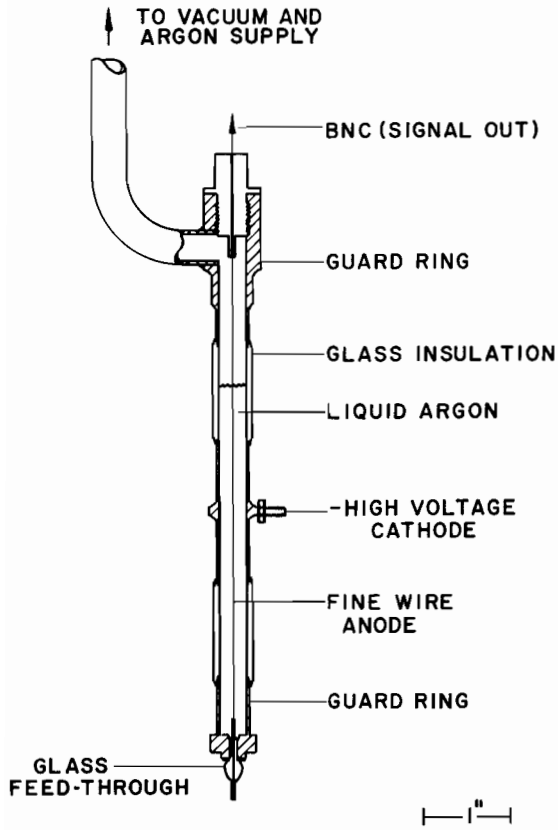

Fig. 2. Typical cylindrical one-wire chamber.

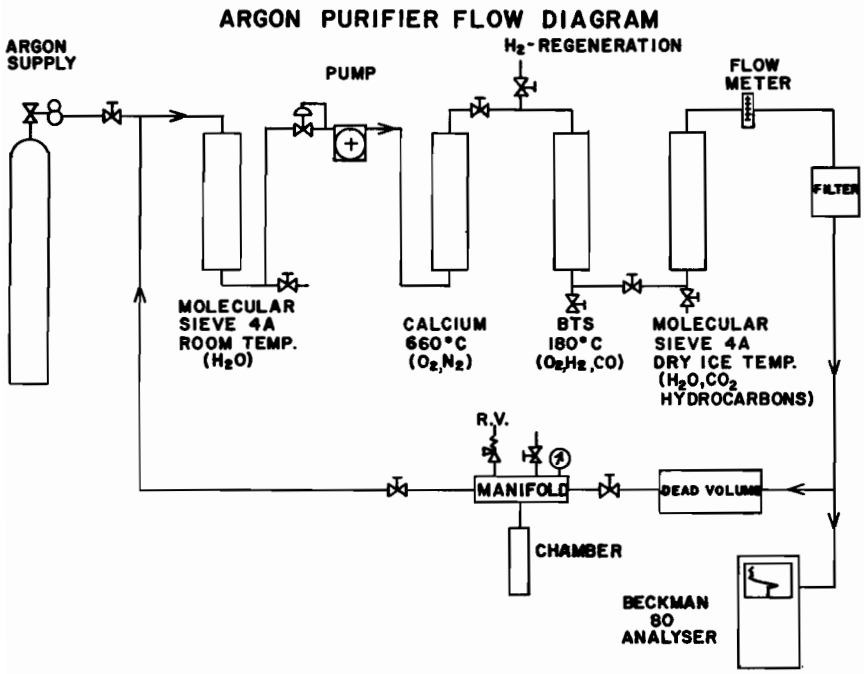

Fig. 3. Argon purifier.

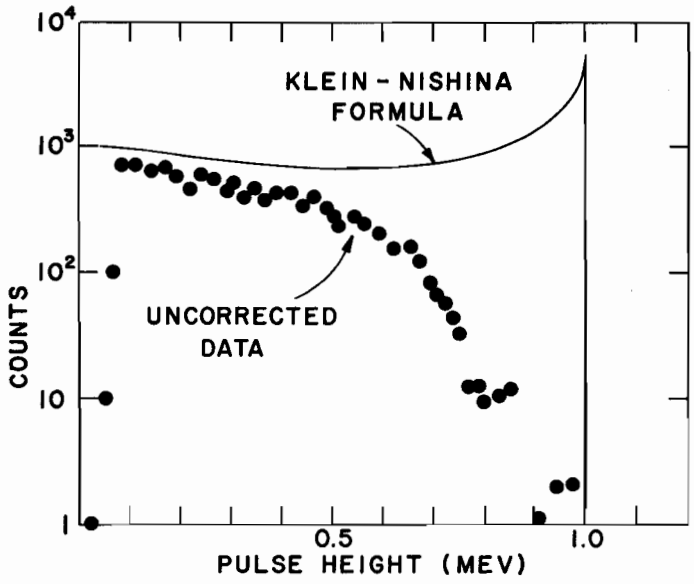

Fig. 4. Pulse-height analysis of ionization pulses in liquid argon. ^{65}Zn source (Compton electrons from 1.1-MeV gamma rays).

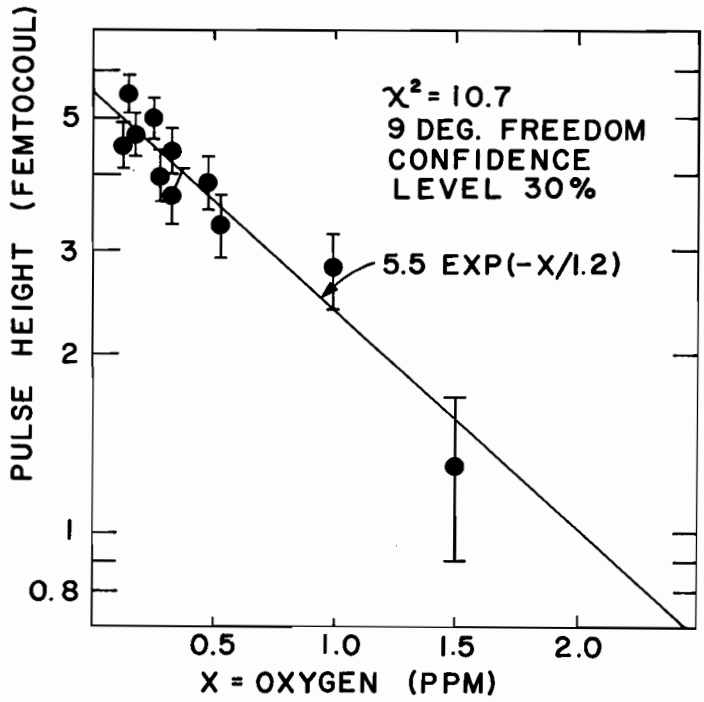

Fig. 5. Ionization pulse height vs oxygen concentration in liquid argon for the chamber shown in Fig. 2 with a 13-μ-diam anode wire and 2000 V potential. ^{65}Zn source.

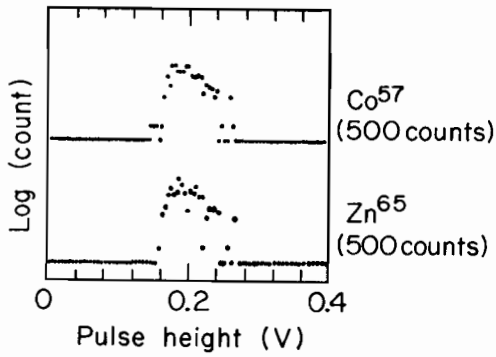

Fig. 6. Comparison of size of avalanche pulses in liquid argon initiated by ^{65}Zn (1.1 MeV gamma rays) and ^{57}Co (120-keV gamma rays) sources.

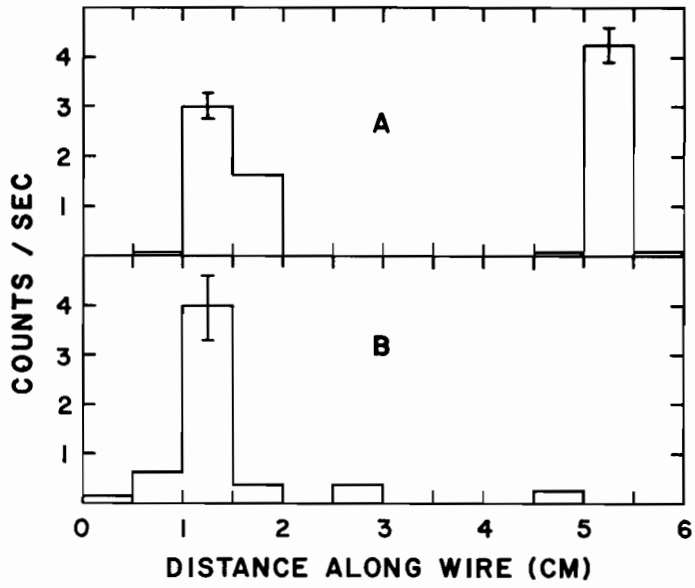

Fig. 7. Count rate in liquid argon. (a) As a 3-mm-diam cylindrical beam of 60-keV x rays from an ^{241}Am source is moved along the wire. (anode: 13-μ-diam stainless steel wire; cathode: 8-mm-diam Kovar cylinder; (b) Same chamber as above after being emptied, warmed, evacuated, and refilled.

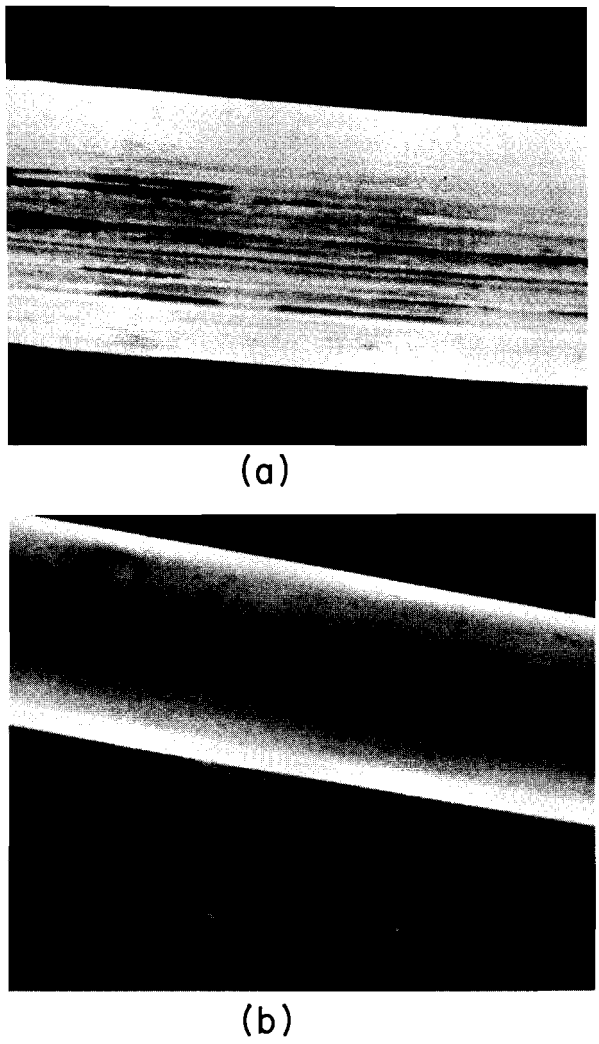

Fig. 8. Scanning electron micrographs of (a) a 0.2-mil tungsten wire and (b) a 0.5-mil stainless-steel wire.

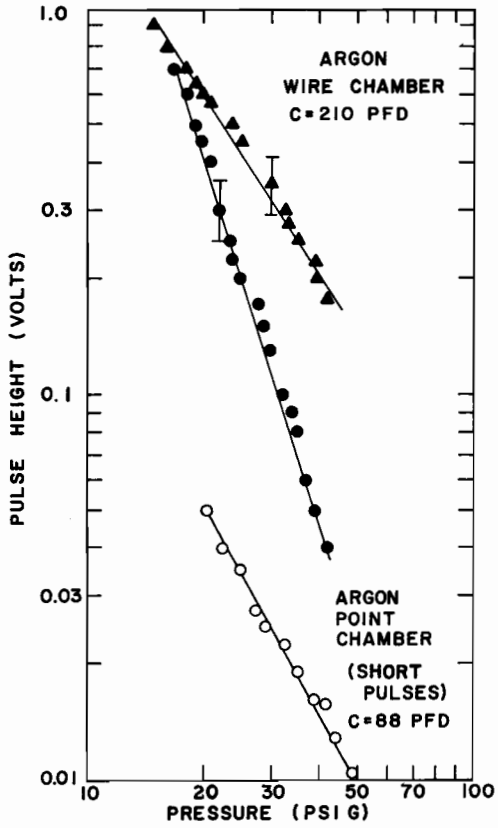

Fig. 9. Pulse height in liquid argon as a function of pressure. The upper curves are for wire chambers, and the lower curve is for a point chamber. Chamber connected directly to an oscilloscope (input impedance 1 MΩ) with a 125-Ω coaxial cable. Total capacitance is indicated.

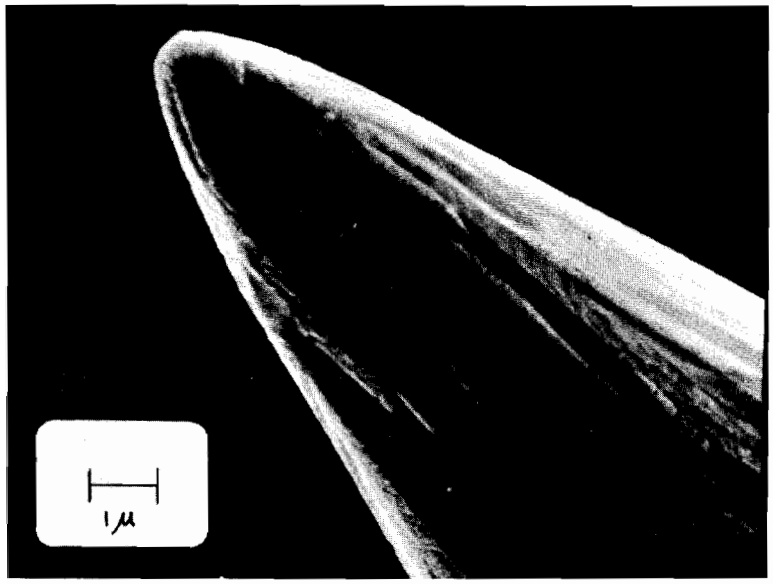

Fig. 10. Scanning electron micrograph of etched tungsten point.

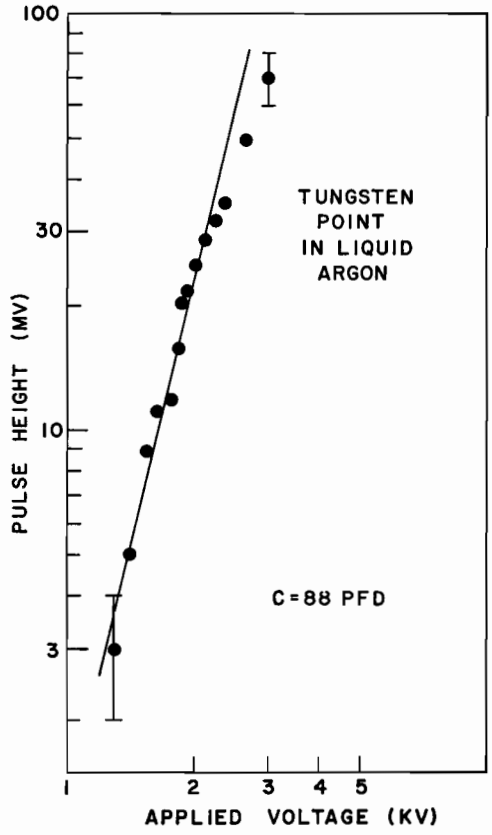

Fig. 11. Pulse height vs voltage for a tungsten point in liquid argon. Chamber connections as described in Fig. 9.

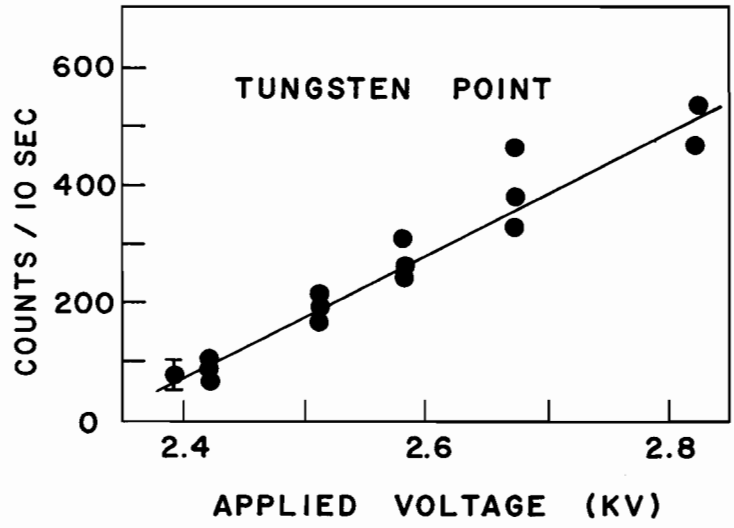

Fig. 12. Count rate vs voltage for a tungsten point in liquid argon. The several points at each voltage indicate the nonstatistical fluctuations that occurred in a run.

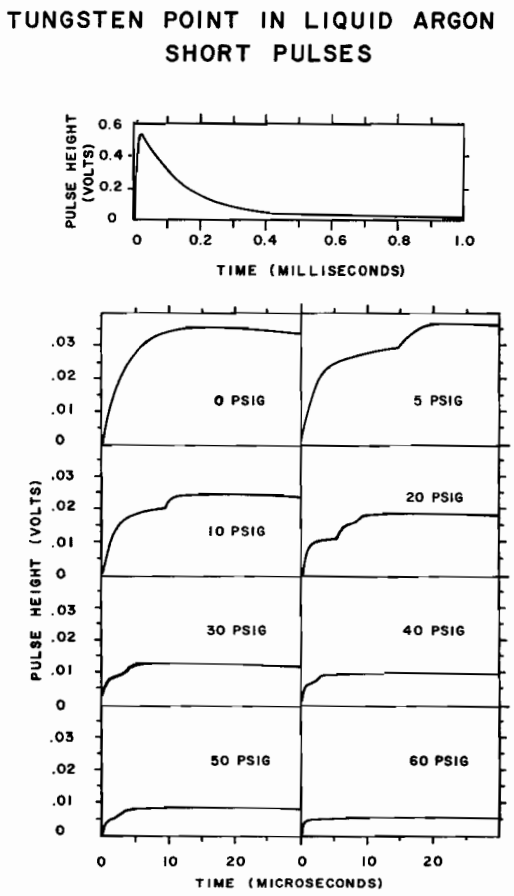

Fig. 13. Pulse shape as a function of pressure for the shorter type of pulse seen in liquid argon on etched tungsten tips.

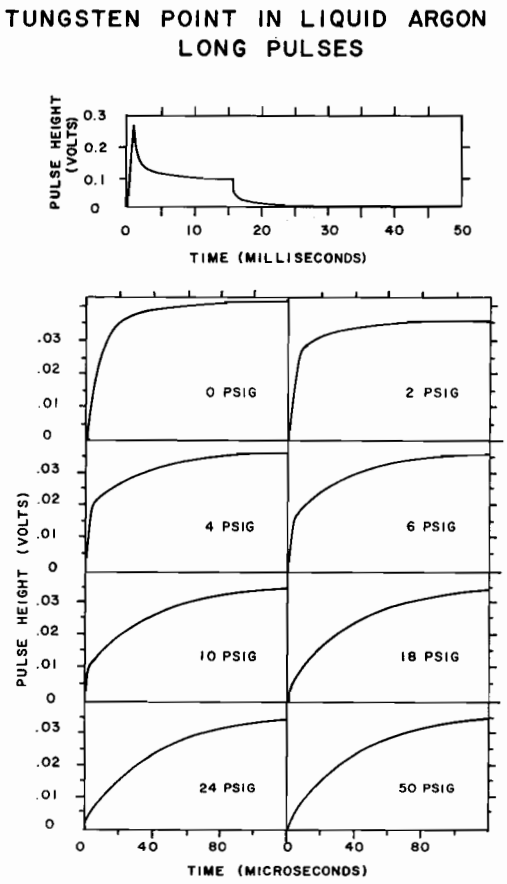

Fig. 14. Pulse shape as a function of pressure for the longer type of pulse seen in liquid argon on etched tungsten tips.

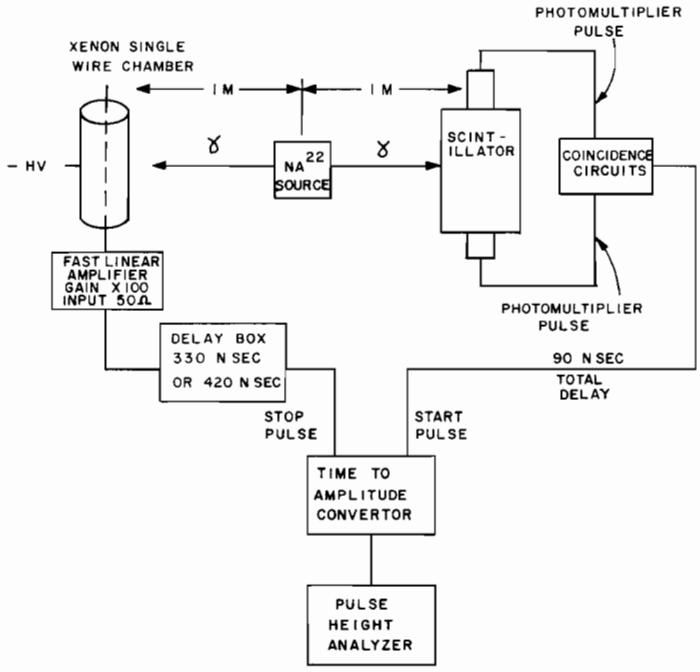

Fig. 15. Apparatus for measurement of time resolution. The liquid xenon chamber pulse was delayed for purposes of display (see following figure).

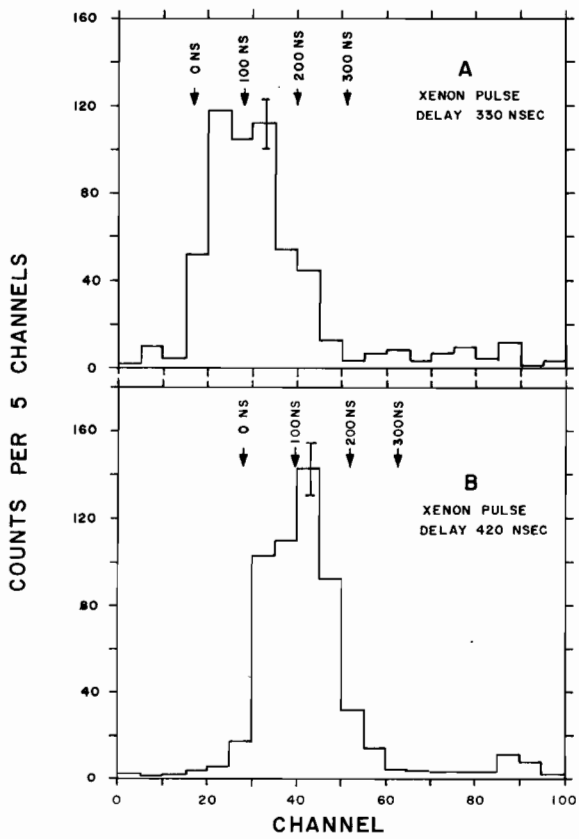

Fig. 16. Distribution of time delays. (a) Between the scintillator and xenon chamber pulses; (b) After the xenon chamber pulses have been delayed an additional 90 nsec; arrows show timing relative to the passage of the Compton electron.

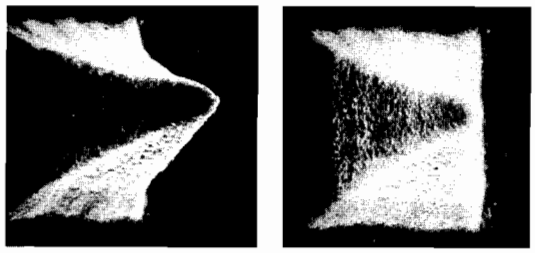

Fig. 17(a). Scanning electron micrograph of deposited pyramids, spaced 25 μ apart.

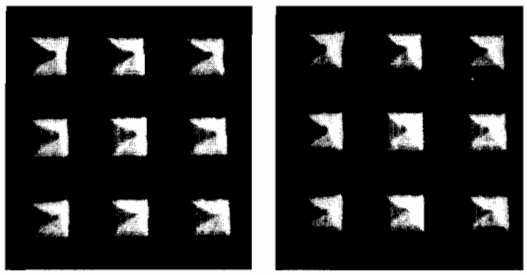

Fig. 17(b). Scanning electron stereo pairs of pyramids. (For best viewing, remove eyeglasses and insert a cardboard septum between the nose and the two pictures so that each eye views only its respective picture.)

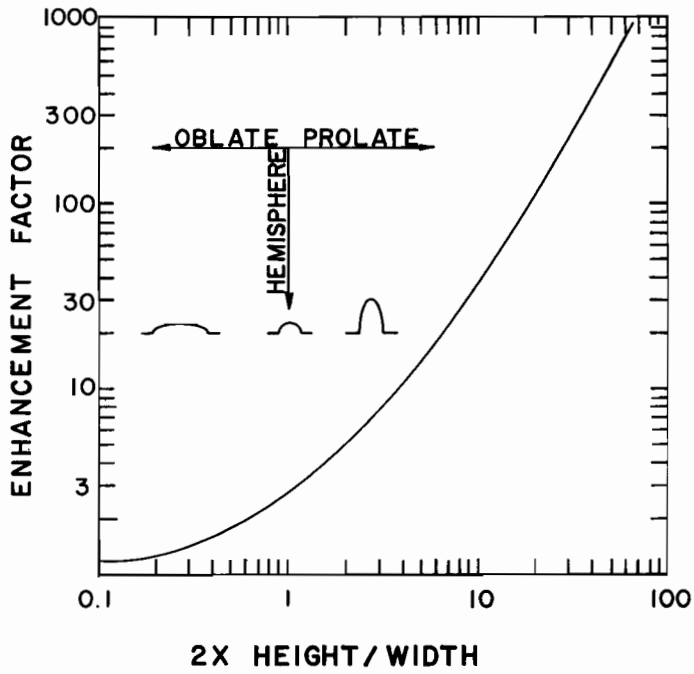

Fig. 18. The electric field enhancement factor for a speroidal structure on a flat plate as a function of the aspect ratio. This factor is defined as the ratio of the maximum field at the surface of the structure to the field that obtains when the structure is removed.